

Fabrication of a Highly Sensitive and Selective Ag-doped WO₃ Formaldehyde Gas Sensor

Xinmin Wang,¹ Chengqun Yu,^{*2} Junxi Wu,² and Yidong Zhang²

¹Zhengzhou College of Animal Husbandry Engineering, Zhengzhou, Henan 450011, P. R. China

²Key Laboratory of Ecosystem Network Observation and Modeling, Institute of Geographic Sciences and Natural Resource Research, Chinese Academy of Sciences, Beijing 100101, P. R. China

(Received March 1, 2012; CL-120170; E-mail: yucq@igsrra.ac.cn)

Ag-doped WO₃ nanowhiskers have been successfully synthesized by a simple sol-gel treatment from the precursors W, H₂O₂, and AgNO₃ at room temperature, followed by heat treatment at 400 °C for 1 h. The samples were characterized by X-ray diffraction (XRD), energy-dispersive spectrum (EDS), and scanning electron microscopy (SEM). Obtained results show that the obtained nanowhiskers width is ca. 200 nm with orthorhombic phase under different Ag-doped concentrations. Compared with the pure WO₃-based sensor, all of the Ag-doped sensors showed better sensing performance in respect of sensitivity and selectivity. The sensor containing 3.0 mol % Ag exhibited the maximum sensitivity to formaldehyde vapor at 150 °C. A possible mechanism for the influence of Ag on the formaldehyde-sensing properties of Ag-doped WO₃ sensors is proposed.

Formaldehyde (HCHO), as a colorless carcinogenic, pungent-smelling gas that can cause some severe symptoms such as watery eyes, nausea, blindness, asthma, and immune system disorders.^{1,2} Therefore, it is necessary to find a portable and low-cost gas detector at home and at the work place for real-time monitoring the levels of HCHO. Presently, some methods have been used to detect HCHO such as biosensors,³ colorimetric detection,⁴ chemiluminescence,⁵ fluorometry,⁶ optical sensors,⁷ and gas sensors.⁸ Particularly, metal-oxide-semiconductor-based gas sensors are promising due to simple working principle, high sensitivity, portability, and low cost.

Tungsten(VI) oxide (WO₃), as a wide band gap n-type semiconductor is a promising sensor because of its excellent sensitivity and selectivity.⁹ It has been shown that a proper amount of metal additives promotes chemical reactions by reducing the activation energy between the film surface and the target gas. Further, it increases the response and selectivity and decreases the maximum temperature of sensor response. Thin WO₃ films were initially used for detecting H₂S, NH₃, and H₂. Thin WO₃ films doped by trace amounts of noble metal (Pd, Pt, Ag, and Au) additive have been found to be more sensitive, selective and show quick response to NO₂, NH₃, and H₂.^{10–12} However, few reports have mentioned noble-metal-doped sensors based on thin WO₃ film to detect HCHO vapor.

Here, we use the precursors W, H₂O₂, and AgNO₃ at room temperature by a sol-gel method to fabricate a Ag-doped WO₃ gas sensor that exhibit high sensitivity and selectivity to HCHO vapor at low concentrations and operating temperatures.

The synthesis of Ag-doped WO₃ particles was carried out by a simple method. Typically, 1.0 g of W powder was slowly added into 30% aqueous H₂O₂ solution (v/v) under fierce stirring. A proper amount of AgNO₃ (1.0, 3.0, and 5.0 mol % ratio) was added into the sol and stirred for 4 h. The sol was transferred into an oven to heat at 120 °C for 4 h, followed by heat treatment at 400 °C for 1 h. All reagents were purchased from Sinopharm Chemical

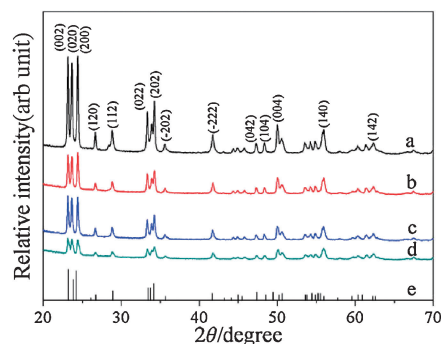


Figure 1. XRD patterns of: (a) pure WO₃ particles, (b) 1.0, (c) 3.0, and (d) 5.0 mol % Ag-doped WO₃ particles, and (e) the standard pattern of WO₃.

Reagent Co., Ltd. (Shanghai, China). The samples of pure WO₃, 1.0, 3.0, and 5.0 mol % Ag-doped particles were marked “a,” “b,” “c,” and “d,” respectively.

The sample was characterized by XRD (Bruker D8 Advance diffractometer) using Cu K α radiation source and SEM (Zeiss EVO LS-15). The gas-sensing performances were investigated by a static gas-sensing system (WS-30A, Weisheng Electronics Co., Ltd., Zhengzhou, China).

An XRD pattern of the resultant Ag-doped WO₃ particles is shown in Figure 1. All the diffraction peaks can be indexed to the orthorhombic phase WO₃ (JCPDS file no. 20-1324). The WO₃ phase was not changed, and the Ag phase was not observed after Ag-doping during the heat treatment, indicating that the Ag crystal particles are effectively penetrated into the WO₃ crystal lattice to form a stable solution. However, compared with the pure WO₃, the intensity of Ag-doped WO₃ diffraction peaks decreased sharply, indicating that the crystallization of Ag-doped WO₃ becomes weak, which suggests that a certain amount of Ag inhibits the crystallization of WO₃. The composition of the obtained Ag-doped WO₃ particles (3.0 mol %, sample “c”) is shown in Figure 2 by EDS analysis. The atomic ratio of W:O is 1:2.78, which did not agree with the stoichiometric ratio in WO₃ (1:3). The deficiency in oxygen revealed substantial oxygen vacancies, which may be introduced during calcinations. No other impurities could be detected except for the doped Ag element and adventitious carbon. In the inset of Figure 2, the SEM images of the pure and Ag-doped WO₃ particles are shown, which displayed nearly the same morphologies of nanowhiskers under different Ag-doping amounts. The average whisker width is ca. 200 nm. Considering that the atomic radii of W and Ag are 202 and 129 pm, respectively, Ag probably penetrated into WO₃ crystal lattice to form a stable solid solution during the heat treatment, which coincides with the XRD pattern.

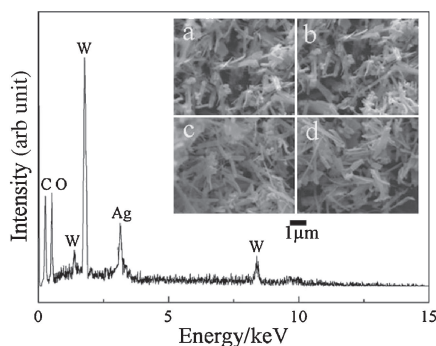


Figure 2. EDS spectrum of sample “c;” (Inset) SEM images of (a) pure WO_3 and (b, c, d) Ag-doped WO_3 particles.

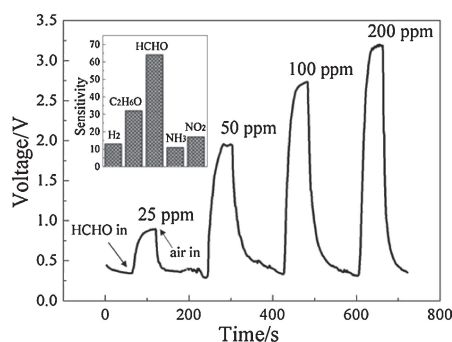


Figure 3. Typical response curves to HCHO vapor under different vapor concentrations at the operating temperature of 150 °C. (Inset) Typical sensitivity values of 3.0 mol % Ag-doped WO_3 -based sensor to various gases at 150 °C.

The sensitivity values to 100 ppm HCHO vapor of samples “a,” “b,” “c,” and “d” were 25.2, 41.8, 64.3, and 43.5, respectively, i.e., the sample “c” with 3.0 mol % Ag doping was the best choice. Figure 3 illustrates the typical response–recovery time curves of the 3.0 mol % Ag-doped WO_3 sensor to different HCHO vapor concentration (from 25 to 200 ppm) at 150 °C. Obviously, the sensitivity to HCHO vapors sharply increases with an increase in vapor concentration. Response and recovery times are the basic parameters of gas sensors, which are defined as the time to reach 90% of the final resistance.¹³ The response and recovery times to 25, 50, 100, and 200 ppm HCHO vapor are 44 and 36 s, 39 and 32 s, 27 and 23 s, 21 and 18 s, respectively. The time is short enough for practical application. For a gas sensor, selectivity is also of great importance for practical applications.¹⁴ Consequently, we examined the sensitivity of 3.0 mol % Ag-doped WO_3 gas sensor to other reducing gases such as H_2 , NH_3 , ethanol, and NO_2 of 100 ppm at 150 °C, as shown in the inset of Figure 3. The sensitivity to HCHO is higher compared with other reducing gas, i.e., selective for HCHO at lower operating temperature.

The gas-sensing mechanism of WO_3 -based sensors belongs to the surface-controlled type, i.e., the resistance change is controlled by the species and amount of chemisorbed oxygen on the surface. The surface layer of WO_3 has a nonstoichiometric structure, which contains oxygen vacancies that can absorb O_2 from air. When O_2 is adsorbed on the sensor surface, it absorbs electrons from the conduction band of WO_3 to produce negatively charged chemisorbed oxygen species such as O_2^- , O^- , and O^{2-} , which created a depletion layer at the surface of WO_3 . As a result, the concentration of electrons in the n-type WO_3 decreases, and hence the

electrical conductance of the material decreases.¹⁵ When HCHO vapors are injected, the interaction of reducing gases with the chemisorbed surface oxygen, which exists in various forms such as O_2^- (abs), O^- (abs), and O^{2-} (abs), can take place in different ways. The HCHO vapor readily reacts with the chemisorbed surface oxygen and thereby releasing electrons back to the conduction band leading to an increase of the electrical conductance of WO_3 . The reaction is as follows: $\text{HCHO} + \text{O}_2^- \rightarrow \text{CO}_2 + \text{H}_2\text{O} + \text{e}^-$.¹⁶ The maximum sensitivity of 3.0 mol % Ag-doped WO_3 sensor to HCHO vapor is probably due to the largest lattice defects and highest surface activity, resulting in stronger interaction between HCHO vapor and the surface active sites. Furthermore, as a noble-metal catalyst, on one hand, Ag can absorb HCHO vapor from environment, leading to the enhanced gas sensitivity. On the other hand, owing to the Fermi level of Ag being higher than that of WO_3 , electrons from Ag are transported to WO_3 to form an accumulation layer at the Ag– WO_3 interface, leading to the decrease of the electrical resistance of WO_3 -based sensor.

In conclusion, the Ag-doped WO_3 nanowhiskers have been successfully synthesized by a simple sol–gel treatment from the precursors of W, H_2O_2 , and AgNO_3 at room temperature followed by heat treatment at 400 °C for 1 h. The pure and Ag-doped WO_3 had nearly uniform nanowhiskers width of ca. 200 nm. Compared with pure WO_3 nanowhiskers, the Ag-doped WO_3 -based gas sensor showed highly sensitive and selective gas-sensing behavior to HCHO vapor. The optimum performance was obtained at an operating temperature of 150 °C for the 3.0 mol % Ag-doped WO_3 -based sensor. The Ag-doped WO_3 nanowhisker-based gas sensor is a promising candidate for application in HCHO monitoring at low temperature.

This work was supported by the Henan Provincial Outstanding Young Science Foundation (No. 074100510018), and Postdoctoral Science Foundation of China (Grant No. 20070410616).

References

- 1 J. A. Pickrell, B. V. Mokier, L. C. Griffis, C. H. Hobbs, A. Bathija, *Environ. Sci. Technol.* **1983**, *17*, 753.
- 2 Y. Herschkovitz, I. Eshkenazi, C. E. Campbell, J. Rishpon, *J. Electroanal. Chem.* **2000**, *491*, 182.
- 3 B. Podola, E. C. M. Nowack, M. Melkonian, *Biosens. Bioelectron.* **2004**, *19*, 1253.
- 4 L. Feng, C. J. Musto, K. S. Suslick, *J. Am. Chem. Soc.* **2010**, *132*, 4046.
- 5 T. Sakai, S.-i. Tanaka, N. Teshima, S. Yasuda, N. Ura, *Talanta* **2002**, *58*, 1271.
- 6 J. Fan, Y. Tang, S. Feng, *Int. J. Environ. Anal. Chem.* **2002**, *82*, 361.
- 7 Y. Mine, N. Melander, D. Richter, D. G. Lancaster, K. P. Petrov, R. F. Curl, F. K. Tittel, *Appl. Phys. B: Lasers Opt.* **1997**, *65*, 771.
- 8 S. Lin, D. Li, J. Wu, X. Li, S. A. Akbar, *Sens. Actuators, B* **2011**, *156*, 505.
- 9 X.-L. Li, T.-J. Lou, X.-M. Sun, Y.-D. Li, *Inorg. Chem.* **2004**, *43*, 5442.
- 10 A. Boudiba, C. Zhang, R. Snyders, M.-G. Olivier, M. Debligny, *Procedia Eng.* **2011**, *25*, 264.
- 11 T. Samerjai, N. Tamaekong, C. Liewhiran, A. Wisitsoraat, A. Tuantranont, S. Phanichphant, *Sens. Actuators, B* **2011**, *157*, 290.
- 12 H. Deng, D. Yang, B. Chen, C.-W. Lin, *Sens. Actuators, B* **2008**, *134*, 502.
- 13 Y. Zhang, Z. Zheng, F. Yang, *Ind. Eng. Chem. Res.* **2010**, *49*, 3539.
- 14 V. D. Kapse, S. A. Ghosh, G. N. Chaudhari, F. C. Raghuvanshi, *Talanta* **2008**, *76*, 610.
- 15 Y. Zhang, G. Jiang, K. W. Wong, Z. Zheng, *Sens. Lett.* **2010**, *8*, 355.
- 16 P. Xu, Z. Cheng, Q. Pan, J. Xu, Q. Xiang, W. Yu, Y. Chu, *Sens. Actuators, B* **2008**, *130*, 802.